

# Dark-field detection method of shallow scratches on the super-smooth optical surface based on the technology of adaptive smoothing and morphological differencing

Chen Li (李晨)<sup>1</sup>, Yongying Yang (杨甬英)<sup>1,\*</sup>, Huiting Chai (柴惠婷)<sup>1</sup>,  
Yihui Zhang (张毅晖)<sup>1</sup>, Fan Wu (吴凡)<sup>1</sup>, Lin Zhou (周林)<sup>1</sup>, Kai Yan (闫凯)<sup>1</sup>,  
Jian Bai (白剑)<sup>1</sup>, Yibing Shen (沈亦兵)<sup>1</sup>, Qiao Xu (许乔)<sup>2</sup>, Hongzhen Jiang (姜宏振)<sup>2</sup>,  
and Xu Liu (刘旭)<sup>2</sup>

<sup>1</sup>State Key Laboratory of Modern Optical Instrumentation, College of Optical Science and Engineering, Zhejiang University, Hangzhou 310027, China

<sup>2</sup>Research Center of Laser Fusion, CAEP, Mianyang 621900, China

\*Corresponding author: chuyyy@zju.edu.cn

Received December 9, 2016; accepted May 18, 2017; posted online June 13, 2017

There exist some shallow scratch defects on the super-smooth optical surface. Their detection has a low efficiency with the existing technologies. So a new detection method, dark-field detection of adaptive smoothing and morphological differencing (DFD-ASMD), is proposed. On one hand, the information of shallow scratches can be kept in dark-field images. On the other hand, their weak characteristics can be separated and protected from being overly reduced during the elimination of noise and background in the image. Experiments show the detection rate of shallow scratches is around 82%, and DFD-ASMD can lay a foundation for quality control of defects on the high-quality optical surface.

OCIS codes: 120.0120, 120.4630, 150.1835, 150.3040.

doi: 10.3788/COL201715.081202.

In recent years, modern optical processing technologies, such as single point diamond turning, ion beam etching, and magneto-rheological finishing, are getting breakthroughs. Machining precisions of super-smooth optics have also been significantly improved<sup>[1-3]</sup>. However, with increasing demands for the optical surface quality, existing precision defect detection technology is often unable to meet the requirements of quality control. Sometimes, there are some special scratch defects on the super-smooth optical surface, and we find that their depth is below 50 nm, which are called shallow scratches in this Letter. Because of their existence, some high precision and high power applications are always under their influence. For instance, in the application of extreme ultraviolet lithography (EUVL), shallow scratches on the optical surface often have some impact on the power spectral density of the surfaces, reducing the accuracy of lithography<sup>[4,5]</sup>. Furthermore, since they can increase the frequency spectrum energy in the width direction<sup>[6]</sup>, the damage threshold value<sup>[7]</sup> of optics will be reduced with the increase of the high power laser's running time<sup>[8]</sup>. Nevertheless, the shallow scratches cannot be detected effectively and quickly through the existing detection technology. And their detection of shallow scratches can improve the optical processing technologies and lay a foundation for the classification of scratches<sup>[9]</sup>.

According to ISO 10110, scratch defects can be detected effectively by visual inspection. The depth of common scratches<sup>[10,11]</sup> observed is between 100–400 nm. Many studies can detect them effectively<sup>[12]</sup>, but there are also

some shallow scratches below 50 nm. Wang *et al.*<sup>[13]</sup> has compared these two kinds of scratches and discovered that the scattering intensity of the shallow scratches is about 20%–50% of that of common scratches with the same width. As a result, shallow scratches are undetected easily under the condition of visual fatigue and the machine vision system<sup>[12]</sup>.

In addition, an atomic force microscope (AFM) can detect the depth of the defects in the nm level, but it has the disadvantages of low detection efficiency and high cost because of its detection method of spot scanning. Moreover, the interference method can also be employed in detecting these scratches. One of the shallow scratches (shown in Fig. 1) can be measured by a white light scanning profiler. But it still can't be used in the rapid detection, with its complex demodulation method and small testing aperture.

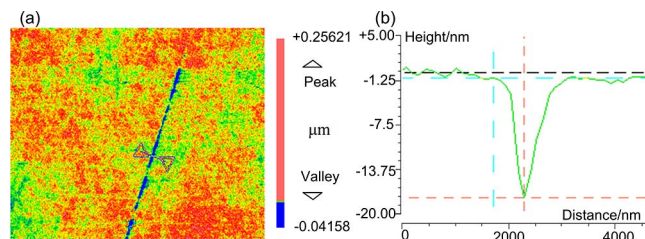


Fig. 1. (a) Measuring result of the shallow scratch on the super-smooth optics; (b) geometrical features of the shallow scratch.

To meet the requirements of effective and fast detection, a new detection method of shallow scratches has been proposed in this Letter. That is a dark-field detection method based on the technology of adaptive smoothing and morphological differencing (DFD-ASMD). First, the optical imaging system only receives the scattered light of defects under the dark-field lighting condition. On one hand, the sensitivity of detection system can be improved<sup>[12,14]</sup>. On the other hand, a large field of view can be formed, and the detection efficiency can also be improved<sup>[15]</sup>. Then, with the use of gray window transformation, the gray values of shallow scratches in the dark-field image are still very low, and it is difficult to separate them from noise and nonuniform background surroundings in the image.

Then, according to the geometric features and imaging features of shallow scratches, the algorithm for adaptive smoothing and morphological differencing (ASMD) has been designed. With the use of gray window transformation, the gray interval, including shallow scratches, can be extracted. Then, according to the differences of shallow scratches, noise, and background in the space field and morphological features, we have designed the adaptive smoothing with a Gaussian filter based on different filter windows and morphological differencing based on the differential threshold. For one thing, noise and background can be eliminated as much as possible. For another, the faint characteristics of shallow scratches can also be protected from being overly reduced during the processing. As a result, the information of shallow scratches can be separated. And then, the total length of scratch defects on the optical surface, can be calculated easily.

First, we attempt to capture the images of shallow scratches utilizing the dark-field imaging principle, which is shown in Fig. 2.

It can be seen from Fig. 2(a) that the CCD, in the condition of lighting with a low angle, can only accept the scattered light of defects, without reflected light. The defect images and background have a high image contrast. Figure 2(b) illustrates that the common scratch with high grayscales in the dark-field, can be easily found. However, the grayscales of the shallow scratch are so low that it cannot easily be separated because of its weak scattered light; but its information can be highlighted with the gray threshold of segmentation reduced, which is shown in Fig. 3.

The information of the shallow scratch does not obviously appear with the gray threshold of  $T'_1 = 60$ . Subsequently, when the gray threshold is reduced to  $T'_2 = 45$ , the information of the shallow scratch appears, but it also is accompanied with background and noise, which will disturb the feature's extraction and calculation of the shallow scratch.

Next, we select three images to analyze their histogram and grayscale distribution, shown as Fig. 4.

Seen from Figs. 4(a) and 4(b), the histogram of the background is very concentrated, and its grayscale distribution seems relatively smooth. The grayscales of the

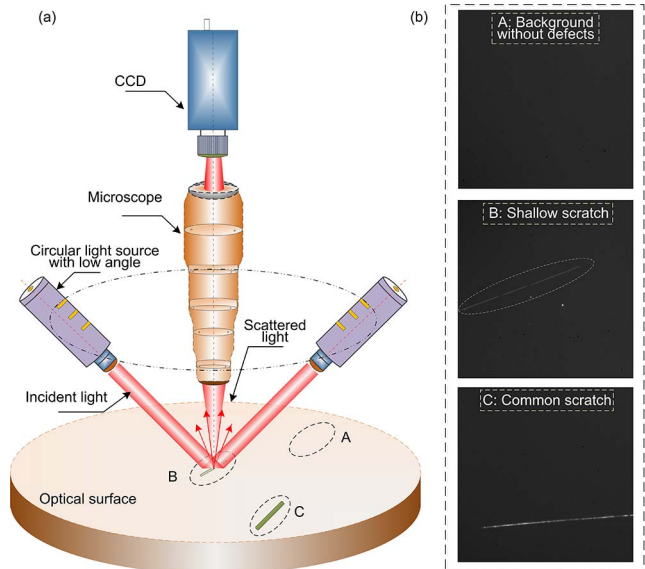


Fig. 2. (a) Schematic of dark-field imaging; (b) dark-field images captured (the grayscales of the shallow scratch have been artificially enhanced to be observed conveniently).

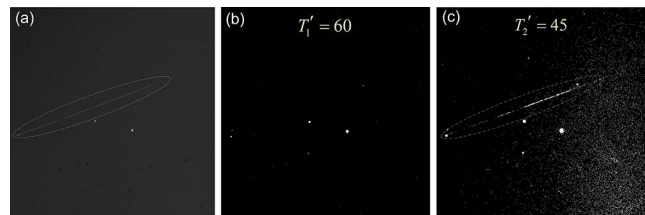


Fig. 3. Results of separating the image with different gray thresholds. (a) Dark-field image including the shallow scratch; (b) the result with  $T'_1 = 60$ ; (c) the result with  $T'_2 = 45$ .

common scratch are concentrated above  $T_1$ , but the grayscale distribution of the image, including the shallow scratch, is similar to that of the background. The grayscales of the shallow scratch are similar to some background surrounding, both of which are distributed between  $T_1$  and  $T_2$ .

Through the analysis above, the information of shallow scratches can be kept in the “mixed grayscales” ( $[T_2, T_1]$ ) of the image with the method of dark-field imaging. Next, a technology of ASMD will be proposed, shown in Fig. 5.

First, the mixed grayscales should be calculated.  $T_1$  and  $T_2$  are the segmentation thresholds of common scratches and most backgrounds, respectively. Assume that the grayscale and pixel ratio of the common defects are  $p_1$  and  $k_1$ . Besides, compared to common defects with high grayscales, shallow scratches and background with very low grayscales can be classified as the same gray level. So, their grayscale and pixel ratio are  $p_2$  and  $k_2$ .  $k_1 < 0.15$  and  $k_2 > 0.85$  are the statistical data. And the grayscale average ( $\bar{T}$ ) and variance ( $\sigma^2$ ) can be expressed as

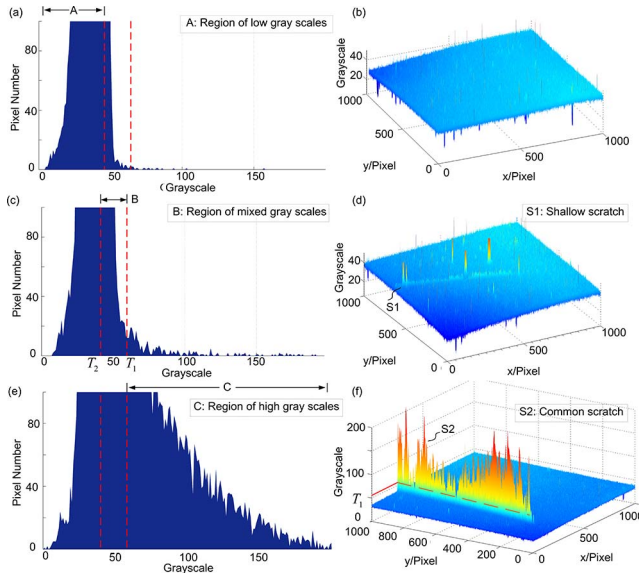


Fig. 4. (a), (c), (e) Partial histogram of background, shallow scratch, and common scratch; (b), (d), (f) grayscale distribution.

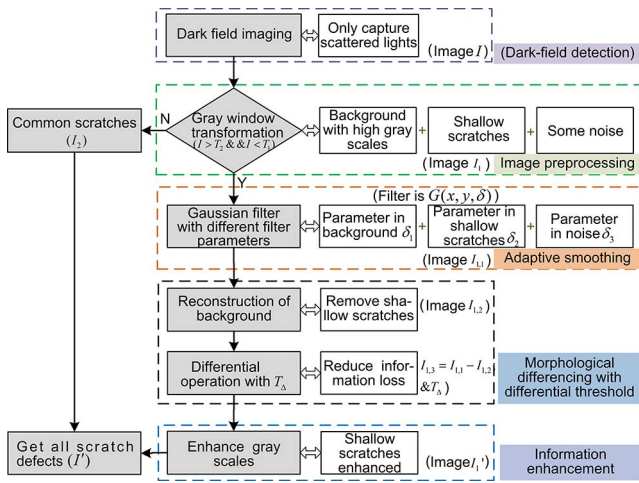


Fig. 5. Flow chart of the ASMD.

$$\begin{cases} \bar{I} = k_1 \times p_1 + k_2 \times p_2 \\ \sigma^2 = k_1(p_1 - \bar{I})^2 + k_2(p_2 - \bar{I})^2, \end{cases} \quad (1)$$

where  $\begin{cases} p_2 < \bar{I} < p_1 \\ 0 < k_1 < k_2 < 1, k_1 + k_2 = 1 \end{cases}$ .

The gray scales ( $p_1, p_2$ ) can be calculated as

$$p_1 = \bar{I} \pm \sqrt{k_2/k_1}\sigma, \quad p_2 = \bar{I} \pm \sqrt{k_1/k_2}\sigma. \quad (2)$$

Because the gray scales of common defects are higher than the grayscale average. So,  $T_1$  can be chosen as  $T_1 = \bar{I} + \sqrt{k_2/k_1}\sigma$ . Inversely,  $T_2$  can be chosen as  $T_2 = \bar{I} - \sqrt{k_1/k_2}\sigma$ . Furtherly, gray intervals ( $[T_2, T_1]$ ) of many dark-field images are calculated to find out the

minimum of  $T_2$  and the maximum of  $T_1$ . And then, they can be used for later applications ( $[0.14, 0.25]$ ).

Then, shallow scratches and some background with noise can be separated with gray window transformation, which is shown as

$$I_1 = \begin{cases} T_2/2, & \text{if } I < T_2 \text{ or } I > T_1 \\ I, & \text{if } T_2 \leq I \leq T_1 \end{cases}. \quad (3)$$

And common defects and most of background can also be eliminated. After the operation, shallow scratches is still mixed with the noise and nonuniform background. Next, ASMD will eliminate different interference and also protect the weak feature of shallow scratches.

To eliminate the noise (Salt and Pepper noise, which is mainly from CCD) in the image ( $I_1$ ), Gaussian filters [ $G(x, y, \delta)$ ] work better. However, if a single filter window is used to smooth the whole image, the weak characteristics of shallow scratches will also be smoothed excessively. Consider that parameter  $\delta$  of the Gaussian filter determines the smoothing degree of the filter to the image, and the width of the Gaussian filter is characterized mainly by parameter  $\delta$ <sup>[10]</sup>. The adaptive Gaussian filter has been designed. That is, different parameters ( $\delta_1, \delta_2, \delta_3$ ) can be calculated to eliminate the noise and protect shallow scratches.

Assume that the grayscale of the pixel to be smoothed is  $\bar{I}_1(x', y')$ , and the gray average of the filter window is  $\bar{I}_1(x', y')$ . Then, the change of the gray value [CGV,  $\Delta f(x', y')$ ] in the filter window can be calculated by

$$\Delta f(x', y') = \left| I_1(x', y') - \bar{I}_1(x', y') \right|. \quad (4)$$

Then, two special assumptions will be discussed. First, the current filter window is located in the region of the background, which is very smooth. And the gray-scales of pixels in the filter window are approximately equal. So,  $\Delta f(x', y') \approx 0$ . The other assumption is that there is only one pixel of noise and its grayscale is higher than others in the window. The higher the grayscale of the noise is, the greater its CGV is. So, the value of  $\Delta f(x', y')$  is inversely proportional to the smoothness of the current filter window and the same as the value  $\delta_{(x', y')}$  of the Gaussian filter. So,  $\delta_{(x', y')}$  can be replaced with  $\Delta f(x', y')$ . Then, the adaptive Gaussian filter will be designed as

$$G_{(x', y')}(i, j) = A e^{-\frac{i^2 + j^2}{2\delta_{(x', y')}^2}}, \quad \text{where } A = \frac{1}{2\pi\delta_{(x', y')}^2},$$

and  $\delta_{(x', y')} = \Delta f(x', y')$ . (5)

To protect the weak information of shallow scratches, a threshold  $T_\delta$  is introduced ( $T_\delta = 3$ , which

can be gotten by statistical calculating), which is shown as

$$\delta_{(x',y')} = \begin{cases} \Delta f(x', y'), & \text{if } \Delta f(x', y') > T_\delta \\ 0.1, & \text{if } \Delta f(x', y') \leq T_\delta \end{cases} \quad (6)$$

$$I_{1,3}(i, j) = \begin{cases} I_{1,1}(i, j) - (I_{1,1} \circ \text{SE})(i, j), & \text{if } I_{1,1}(i, j) - (I_{1,1} \circ \text{SE})(i, j) < T_\Delta \\ I_{1,1}(i, j), & \text{if } I_{1,1}(i, j) - (I_{1,1} \circ \text{SE})(i, j) \geq T_\Delta \end{cases} \quad (8)$$

Equation (6) reveals that if  $\Delta f(x', y') > T_\delta$ , the current filter window can be judged to locate in the region of the noise. Then, the noise can be smoothed largely by replacing parameter  $\delta_{(x',y')}$  with CGV. Also, the parameter  $\delta_{(x',y')}$  of the Gaussian filter is set to 0.1 in the region of the background or shallow scratch, and the current filter window will not be smoothed.

After the adaptive smoothing, there is also some non-uniform background. Consider that the size of the shallow scratches is smaller than that of the nonuniform background. And the opening operation is used to remove small bright pixels<sup>[17]</sup>. So, the background ( $I_{1,2}$ ) can be separated, and the image only containing shallow scratches can be separated by the subtraction. In general, the size of the selected structuring element ( $9 \times 9$ ) in the opening operation is less than the size of the background and larger than the width of shallow scratches.

Besides, the image size of large fine optics is always so huge that morphological operations will cost much time. In order to improve its efficiency, structuring element SE is decomposed into two smaller ones<sup>[18]</sup>. So, the operation above is shown as

$$I_{1,3} = I_{1,1} - I_{1,2} = I_{1,1} - I_{1,1} \circ \text{SE} = I_{1,1} - I_{1,1} \circ (\text{SE}_1 \oplus \text{SE}_2) = I_{1,1} - [(I_{1,1} \circ \text{SE}_1) \circ \text{SE}_2], \quad (7)$$

where  $\circ$  and  $\oplus$  are morphological opening and closing operations.

However, there are some gray values at the position of the shallow scratch. After the differencing operation, the grayscale of the shallow scratch are reduced, and the contrast of the image is also very low. To solve these problems, a differential threshold ( $T_\Delta$ ) will be added ( $T_\Delta = 2$ , which can be gotten by statistical calculating).

Then, the shallow scratch with gray jump can be reserved during morphological differencing, which is shown as

Through the operation above, image  $I_{1,3}$ , containing only shallow scratches, can be extracted. The whole processing of DFD-ASMD is shown as Fig. 6.

It can be seen from Fig. 6(f) that the useless information out of the interval in region A can be decreased by gray window transformation. With the method of adaptive smoothing, the noise in region B can be largely smoothed, which is shown as Fig. 6(g). And the weak information of shallow scratch cannot be smoothed excessively in the Fig. 6(c). Furthermore, the nonuniform background in Fig. 6(b) can be eliminated through the operation of morphological differencing. In addition, by comparing Figs. 6(c) and 6(d), the contrast of the image of the

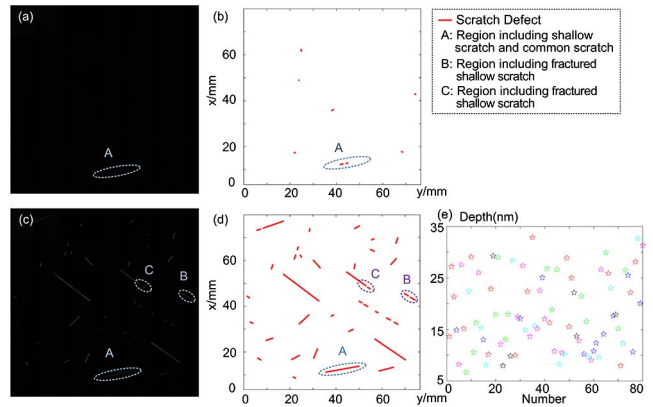


Fig. 7. (a) Dark-field image without using the ASMD; (b) the positions of scratches contained in (a) are marked by SDES; (c) the dark-field image after using the ASMD; (d) the positions of scratches contained in (c). The  $6 \times 6$  images are located on different optical surfaces. We just stitch them to conveniently calculate the total length of scratches. (e) Depth of shallow scratches. Depths above 10 nm can be detected effectively, while some shallow scratches (near 5 nm) cannot be detected.

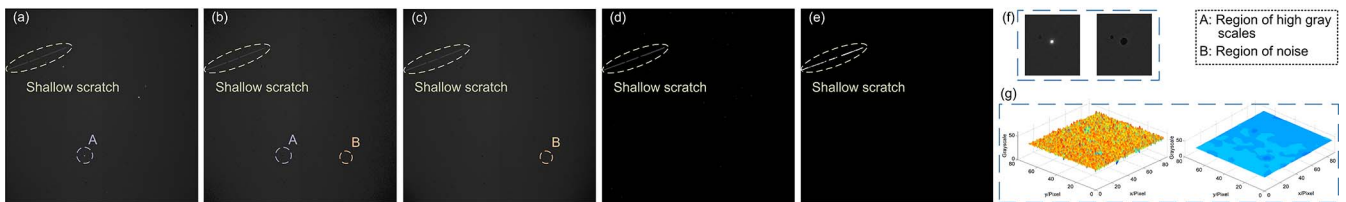


Fig. 6. (a) Image of optical surface gotten by the dark-field detection method; (b)–(d) results of the ASMD; (e) result of gray stretching; (f) result of ASMD in region A; (g) result of ASMD in region B.

**Table 1.** Results of Scratch Detection With or Without ASMD

	SDES without using ASMD	SDES using ASMD	Visual inspection
The size of region detected	The number of images is $6 \times 6$ , and field of view of each image is about $15 \times 15$ mm.		
Total length	3.73 mm	138.42 mm	162.75 mm
Detection rate	2.29%	85.05%	

shallow scratch and background surrounding has been enhanced. Finally, the weak information of the shallow scratch can be enhanced to the “common” scratch by gray stretching. Now, DFD-ASMD is applied into the surface defects evaluation system (SDES)<sup>[15]</sup>.

As is shown in region A of Fig. 7(b), SDES can detect parts of the scratch defects, most of which are common scratches. The shallow scratch included in region A cannot be detected effectively. And the total length of scratches included in Fig. 7(a) is 3.73 mm, which is calculated by SDES. However, with the method of ASMD, shallow scratches included in each sub-image have been enhanced and can be easily recognized. And the total length of scratches is 138.42 mm.

Further, the regions on the optical surfaces, which correspond to the dark-field images shown in Fig. 7, are re-detected by careful visual inspection. The results are shown as Table 1. The actual length of the scratches can also be calculated by AFM. But it will cost much more time so that it isn't suitable to the detection for a large size of region. So, we regard total length calculated by careful visual inspection as the actual length, according to the ISO 10110. For the images of shallow scratches shown as Fig. 7, if the ASMD is added in SDES, the detection rate of scratches can be increased to about 85%. Moreover, taking no account of common scratches, the detection rate of shallow scratches is around 82%.

However, because of nonuniform illumination or reflected light of the environment, the grayscales of fractured shallow scratches of regions B and C in Fig. 7(c) and 7(d) (the depth of them is near 5 nm) are approximately equal to the grayscales of background surrounding, so it may be judged as the background. And SDES has calculated the length of two parts of the fractured shallow scratches, respectively, resulting that the length calculated is lower than the actual length. Some studies can be done to improve the detection rate of scratch defects in the future, such as optimizing the design of lighting.

In conclusion, a new and effective detection of shallow scratches is proposed in this Letter (DFD-ASMD). A dark-field imaging technology is employed to keep the information of shallow scratches in a gray interval of the dark-field image. However, they are still difficult to be separated from noise and nonuniform background. Therefore, based on the differences of different information in the space field and morphological features, ASMD is also designed. On one hand, noise and background can be eliminated. On the other hand, the weak characteristics of

shallow scratches can also be protected from being overly reduced. As a result, shallow scratches can be separated from the original dark-field images and can be merged into the total scratch defects with the common scratches on the optical surface. In the experiments, the detection rate of shallow scratches is around 82%. DFD-ASMD can be used to improve the capacity of existing detection technology for scratch defects and can lay a foundation for quality control of defects on the high-quality optical surface.

This work was supported by the National Natural Science Foundation of China (Nos. 61627825 and 11275172) and the State Key Laboratory of Modern Optical Instrumentation Innovation Program (MOI) (No. MOI2015 B06).

## References

- Q. Xu, J. Wang, W. Li, X. Zeng, and S. Jing, in *International Symposium on Industrial Lasers* (1999), p. 236.
- W. Liu, C. Wei, K. Yi, and J. Shao, *Chin. Opt. Lett.* **13**, 041407 (2015).
- J. Chen, X. Xu, C. Wei, M. Yang, J. Gu, and J. Shao, *Chin. Opt. Lett.* **13**, 032201 (2015).
- P. Yan, *Handbook of Photomask Manufacturing Technology* (CRC Press/Taylor & Francis Information Group, 2005).
- M. Sugawara, I. Nishiyama, K. Motai, and J. Cullins, *Jpn. J. Appl. Phys.* **45**, 9044 (2006).
- R. Huan, J. Hongzhen, and L. Xu, *High Power Laser Part. Beams* **26**, 26092011 (2014).
- P. Cao, Y. Yang, C. Li, H. Chai, Y. Li, S. Xie, and D. Liu, *Chin. Opt. Lett.* **13**, 041102 (2015).
- L. R. Baker, *Metrics for High-Quality Specular Surfaces* (SPIE Press, 2004), Vol. **65**.
- R. K. Kimmel and R. E. Parks, *ISO 10110 Optics and Optical Instruments: Preparation of Drawings for Optical Elements and Systems: A User's Guide* (Optical Society of America, 2002).
- Y. Wang, Q. Xu, L.-Q. Chai, N. Chen, and X.-Q. Zhu, *High Power Laser Part. Beams* **17**, 67 (2005).
- J. Bennett, D. Burge, J. Rahn, and H. Bennett, in *Technical Symposium East* (1979), p. 124.
- Y. Yang, C. Lu, J. Liang, D. Liu, L. Yang, and R. Li, *Acta Opt. Sin.* **27**, 1031 (2007).
- S. Wang, Y. Yang, L. Zhao, H. Chai, D. Liu, J. Bai, and Y. Shen, *Chin. J. Lasers* **42**, 0708005 (2015).
- J. S. Batchelder and M. A. Taubenblatt, “Dark Field Imaging Defect Inspection System for Repetitive Pattern Integrated Circuits,” U.S. patent 5,177,559 (January 5, 1993).
- D. Liu, Y. Yang, L. Wang, Y. Zhuo, C. Lu, L. Yang, and R. Li, *Opt. Commun.* **278**, 240 (2007).
- I. T. Young and L. J. Van Vliet, *Signal Process.* **44**, 139 (1995).
- A. M. Mendonca and A. Campilho, *IEEE Trans. Med. Imaging* **25**, 1200 (2006).
- H. Park and J. Yoo, *IEE Proc. Vis. Image Signal Process.* **148**, 31 (2001).